Large Size LYSO Crystals for Future High Energy Physics Experiments

Jianming Chen, *Member, IEEE*, Liyuan Zhang, *Member, IEEE*, and Ren-Yuan Zhu, *Senior Member, IEEE*

***Abstract*—Because of their high stopping power and fast bright scintillation, cerium doped silicate based heavy crystal scintillators, such as GSO, LSO, and LYSO, have been developed for medical instruments. Their applications in high energy and nuclear physics, however, are limited by lacking high quality crystals in sufficiently large size. The optical and scintillation properties, including the transmittance, emission and excitation spectra and the light output, decay kinetics and light response uniformity, as well as their degradation under γ-ray irradiation were measured for two long ($2.5 \times 2.5 \times 20$ cm) LYSO samples from CPI and Saint-Gobain, and were compared to a BGO sample of the same size from SIC. Possible applications for crystal calorimetry in future high energy and nuclear physics experiments are discussed.**

***Index Terms*—Crystal, emission, light output, lutetium oxyorthosilicate, lutetium yttrium oxyorthosilicate, radiation damage, scintillator, transmission.**

I. Introduction

In the last decade, cerium doped silicate based heavy crystal scintillators have been developed for the medical industry. As of today, mass production capabilities of Gadolinium Orthosilicate (Gd_2SiO_5, GSO) [1], lutetium oxyorthosilicate (Lu_2SiO_5, LSO) [2] and lutetium-yttrium oxyorthosilicate ($Lu_{2(1-x)}Y_{2x}SiO_5$, LYSO) [3], [4] are established. Table I lists basic properties of commonly used heavy crystal scintillators: NaI(Tl), CsI(Tl), undoped CsI, BaF_2, bismuth germanate ($Bi_4Ge_3O_{12}$ or BGO) and lead tungstate ($PbWO_4$ or PWO) as well as cerium doped GSO and LSO. All these crystal scintillators, except LSO and GSO, have been used in high energy or nuclear physics experiments. An early example is a Crystal Ball NaI(Tl) calorimeter at SPEAR. CsI(Tl) crystals were used for calorimeters of CLEO at CESR, *BABAR* at SLAC and BELLE at KEK. KTeV built a CsI calorimeter at the Tevatron, and a BGO calorimeter was built by L3 at the LEP. BaF_2 crystals were used in the TAPS experiment at GSI. Recently, PWO crystals are used by CMS and Alice at the LHC and by CLAS and PrimEx at CEBAF.

Because of their high stopping power and fast bright scintillation light, cerium doped silicate has also attracted a broad interest in the physics community. The main obstacles of using these crystals in the experimental physics are two fold: the availability of high quality crystals in sufficiently large size and the high cost associated with their high melting point ($\sim$2 000°C). Recent emergence of large size LYSO crystals in the market, however, inspired this investigation on possible applications of this new generation scintillators in experimental physics, such as a super B factory [5].

Manuscript received April 1, 2005.

This work was supported in part by the U.S. Department of Energy under Grant DE-FG03-92-ER40701.

The authors are with the California Institute of Technology, Pasadena, CA 91125 USA (e-mail: zhu@hep.caltech.edu).

Digital Object Identifier 10.1109/TNS.2005.862923

II. Samples and Experimental Apparatus

Fig. 1 is a photo showing three long crystal samples with dimension of $2.5 \times 2.5 \times 20$ cm. They are, from top to bottom: BGO samples from Shanghai Institute of Ceramics (SIC) and LYSO samples from Crystal Photonics, Inc. (CPI) and Saint-Gobain Ceramics & Plastics, Inc. (Saint-Gobain). While the SIC and Saint-Gobain long samples have perfect geometry and surface polishing, the CPI long sample has chips at the corners and surfaces as shown in Fig. 1. This is due to the fact that CPI does not have adequate polishing and thermal treatment facilities for such large size samples. Also shown in Fig. 1 are two small cube samples each with dimension of 1.5 radiation length ($1.7 \times 1.7 \times 1.7$ cm) from these three vendors. In addition, two small LSO cube samples of the same size from CTI were also investigated. All long samples are referred to -L, such as SIC-L, in this paper.

According to the manufactures, the yttrium content is about 5% for the CPI LYSO [6] and about 10% for the Saint-Gobain LYSO [7]. The nominal cerium doping level is 0.2% for the CTI LSO [8] and the CPI LYSO [6], and is less than 1% for the Saint-Gobain LYSO [7]. The actual cerium concentration in these crystals, however, would be less than the nominal value and its distribution along the long sample's axis also varies because of the segregation. The technical nature of long crystal's ends, such as the seed or tail in growth, however, are not provided by the manufactures.

All surfaces of these samples are polished. No thermal treatment was applied before initial measurements. The transmittance spectrum was measured by using a Hitachi U-3210 UV/visible spectrophotometer with double beam, double monochromator and a large sample compartment equipped with a custom Halon coated integrating sphere. The systematic uncertainty in repeated measurements is about 0.3%. Taking into account multiple bouncing between two end surfaces, the theoretical limit of transmittance without internal absorption, T_s, can be calculated as [9]

$$T_s = (1-R)^2 + R^2(1-R)^2 + \cdots = (1-R)/(1+R) \quad (1)$$

where

$$R = \frac{(n_{\text{crystal}} - n_{\text{air}})^2}{(n_{\text{crystal}} + n_{\text{air}})^2}. \quad (2)$$

TABLE I
PROPERTIES OF SOME HEAVY CRYSTAL SCINTILLATORS

Crystal	NaI(Tl)	CsI(Tl)	CsI	BaF_2	BGO	PWO	LSO(Ce)	GSO(Ce)
Density (g/cm^3)	3.67	4.51	4.51	4.89	7.13	8.3	7.40	6.71
Melting Point (°C)	651	621	621	1280	1050	1123	2050	1950
Radiation Length (cm)	2.59	1.86	1.86	2.03	1.12	0.89	1.14	1.38
Molière Radius (cm)	4.13	3.57	3.57	3.10	2.23	2.00	2.07	2.23
Interaction Length (cm)	42.9	39.3	39.3	30.7	22.8	20.7	20.9	22.2
Refractive Index[a]	1.85	1.79	1.95	1.50	2.15	2.2	1.82	1.85
Hygroscopicity	Yes	slight	slight	No	No	No	No	No
Luminescence[b] (nm) (at Peak)	410	560	420 310	300 220	480	560 420	420	440
Decay Time[b] (ns)	230	1250	35 6	630 0.9	300	30 10	40	60
Light Yield[b,c]	100	45	5.6 2.3	21 2.7	14	0.4 0.1	75	30
d(LY)/dT[b,d] (%/°C)	∼0	0.3	-0.6	-2 ∼0	-1.6	-1.9	-0.3	-0.1

a At the wavelength of the emission maximum.
b Top line: slow component, bottom line: fast component.
c Relative and measured with a PMT with a Bi-alkali cathode.
d At room temperature.

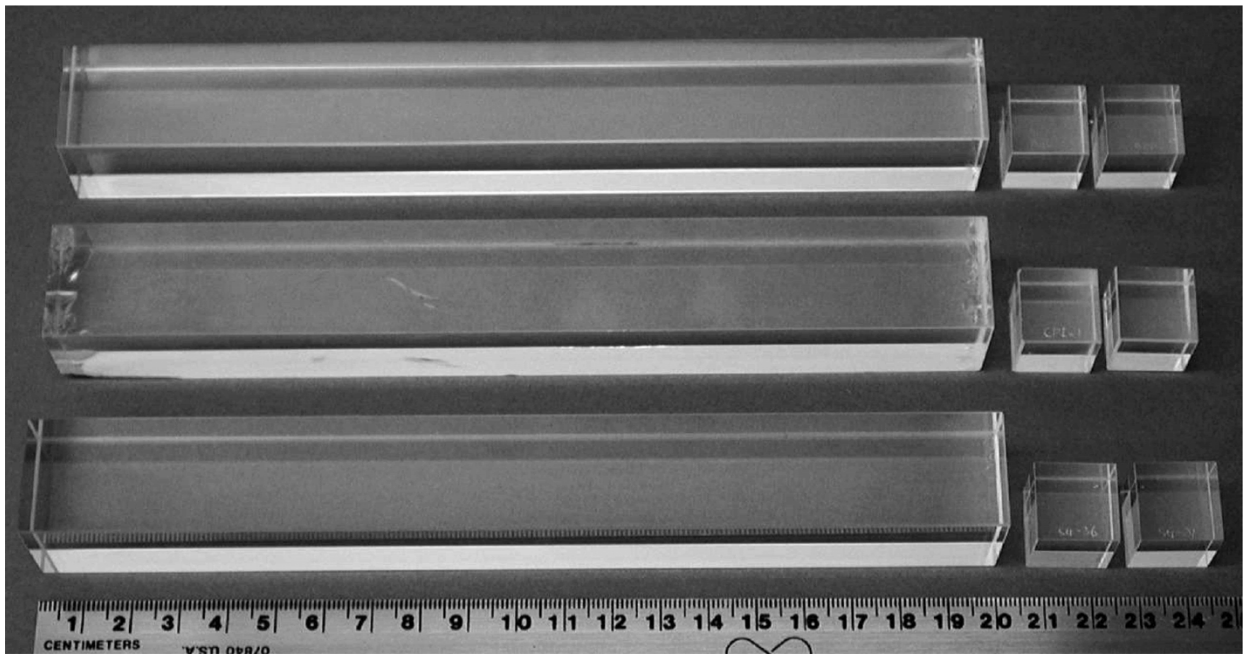

Fig. 1. Photo showing one long (2.5 × 2.5 × 20 cm) crystal samples and two cubes (1.7 × 1.7 × 1.7 cm) each from three vendors. From top to bottom: SIC BGO, CPI LYSO, and Saint-Gobain LYSO.

A comparison of the measured transmittance and T_s may reveal internal absorption.

The excitation, photo luminescence and radiation induced phosphorescence spectra were measured using a Hitachi F-4500 fluorescence spectrophotometer. For the excitation and emission spectra, a UV excitation light was shot to a bare surface of the sample, and the crystal was oriented so that its surface normal is at an angle θ with respect to the excitation light. A positive θ indicates that the photoluminescence emission light is not affected by sample's internal absorption.

The scintillation light output and decay kinetics were measured using a Photonis XP2254b PMT, which has a multi-alkali photo cathode and a quartz window. For measurements of the light output one end of a sample was coupled to the PMT with the Dow Corning 200 fluid, while all other faces of the sample were wrapped with the Tyvek paper. A collimated ^{137}Cs source was used to excite the sample. The γ-ray peak was obtained by a simple Gaussian fit. A Hamamatsu R1306 PMT with bialkali photo cathode and high quantum efficiency was used to measure the ^{137}Cs peak energy resolution for these samples.

The light output of long samples was measure by shooting a collimated ^{137}Cs γ-ray source at seven evenly distributed locations along crystal's longitudinal axis. The light output responses at these seven points were fit to a linear function

$$\frac{\mathrm{LO}}{\mathrm{LO}_{\mathrm{mid}}} = 1 + \delta(x/x_{\mathrm{mid}} - 1) \tag{3}$$

where $\mathrm{LO}_{\mathrm{mid}}$ represents the light output at the middle of the sample, δ represents the deviation of the light response uniformity, and x is the distance from the end coupled to the readout device. Because these samples have a rectangular shape, there are two ways to couple it to the PMT. We define the A end such

TABLE II
IRRADIATION TIME AND THE INTEGRATED DOSAGE APPLIED TO TWO LONG LYSO SAMPLES

Sample	Under 2 rad/h		100 rad/h		9,000 rad/h	
CPI	24 h	48 rad	24 h	2,400 rad	22 h	198 krad
Saint-Gobain	19 h	38 rad	19 h	1,900 rad	22 h	198 krad

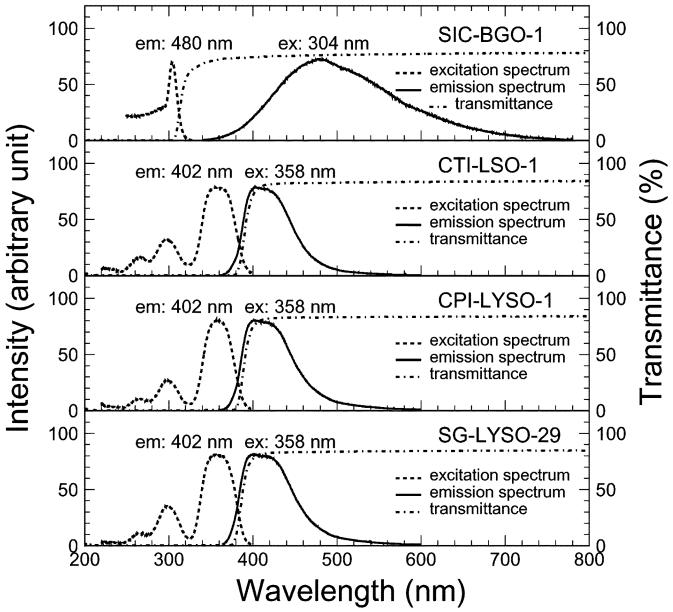

Fig. 2. Optical properties are shown as a function of wavelength for four cube samples. The excitation and emission spectra correspond to the left vertical scale, and the transmittance spectra to the right.

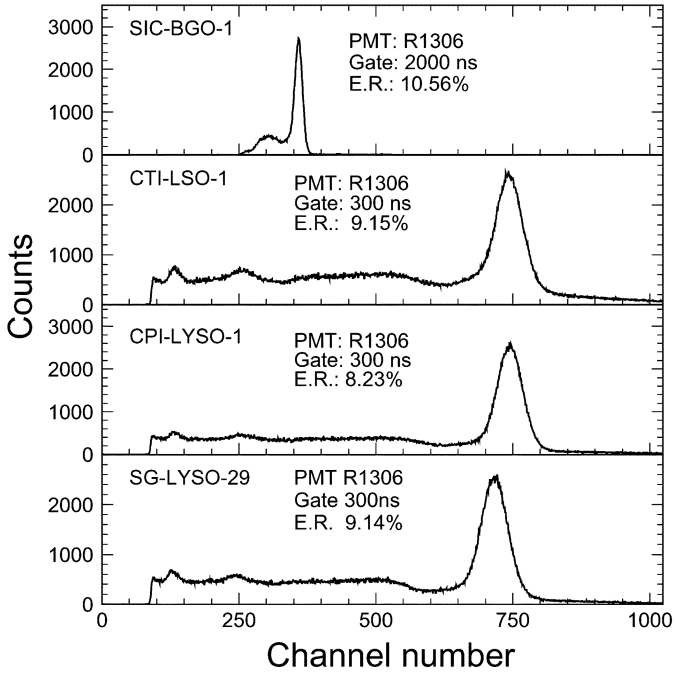

Fig. 3. ^{137}Cs pulse height spectra measured with the R1306 PMT are shown for four cube samples.

that the sample produces a lower average light $(\mathrm{LO}_{\mathrm{mid}})$ when it was coupled to the PMT. The other end is defined as the B end.

The degradation of these optical and scintillation properties of two long LYSO samples under γ-ray irradiations was investigated at two irradiation facilities at Caltech: an open 50 curie ^{60}Co source and a closed 2 000 curie ^{137}Cs source. The former provides dose rates of 2 and 100 rad/h by placing samples at appropriate distances. The later provides a dose rates of 9 000 rad/h with 5% uniformity when samples are placed at the center of the irradiation chamber. Irradiations were carried out step by step with dose rates of 2, 100, and 9 000 rad/h. Table II lists irradiation time and corresponding integrated dosage applied to two long LYSO samples in each step. The radiation induced phosphorescence in these long LYSO samples was also measured as the anode current of a Hamamatsu R2059 PMT with its quartz window coupled to the sample after irradiations under 9 000 rad/h.

III. SCINTILLATION AND OPTICAL PROPERTIES OF THE CUBE SAMPLES

Fig. 2 shows a comparison of the transmittance (right scale), emission and excitation spectra as a function of wavelength for four cube samples: a SIC BGO, a CTI LSO and two LYSO samples from CPI and Saint-Gobain. One notes that the LSO and LYSO samples have identical transmittance, excitation and emission spectra. It is also interesting to note that the emission spectra of the LSO and LYSO samples overlaps with their absorption edge in their transmittance, while the emission of the BGO sample is well within its transparent wavelength region. This overlap of transmittance and emission spectra, which is much more clearly seen in the long samples, indicates that the light output of the LSO and LYSO samples is affected by their intrinsic absorption. Alternatively, an improvement of the transmittance in the direction of a shorter wavelength would effectively improve the light output for LSO and LYSO crystals. This kind of improvement has been achieved in previous crystal development programs for high energy physics. One recent example is the lead tungstate crystal development for the CMS experiment at LHC [10].

Fig. 3 shows a comparison of self-triggered ^{137}Cs pulse height spectra measured for four cube samples coupled to the R1306 PMT. The FWHM resolution of the ^{137}Cs peak is 8 to 9% for LSO and LYSO and 10% for BGO. This resolution is compatible with what obtained by commercially available pixel crystals of much smaller size.

Fig. 4 shows a comparison of light output and decay kinetics observed for four cube samples coupled to the XP2254b PMT. One notes that the LSO and LYSO samples have consist decay time and photoelectron yield. While the 300 ns decay time of the BGO sample is a factor of 7 slower, its measured photoelectron yield is a factor of 6 lower than that of the LSO and LYSO samples. Fig. 5 shows the quantum efficiency of the XP2254b PMT used to measure the light output and decay kinetics. Also shown in the figure are the emission spectra for LSO/LYSO and BGO

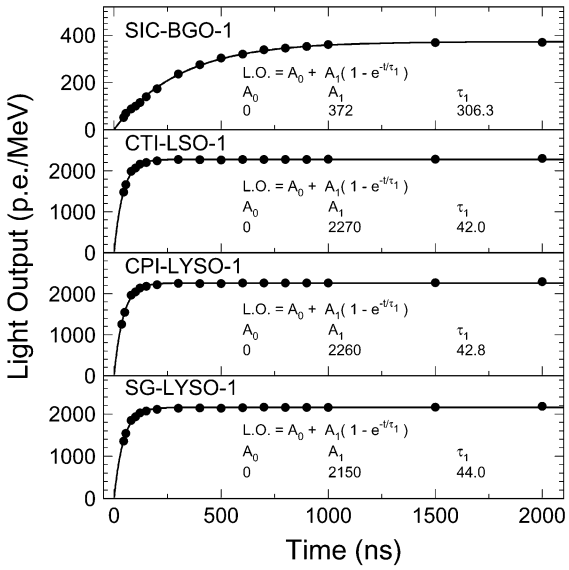

Fig. 4. Light output and decay kinetics measured using the XP2254b PMT are shown as a function of the integration time for four cube samples.

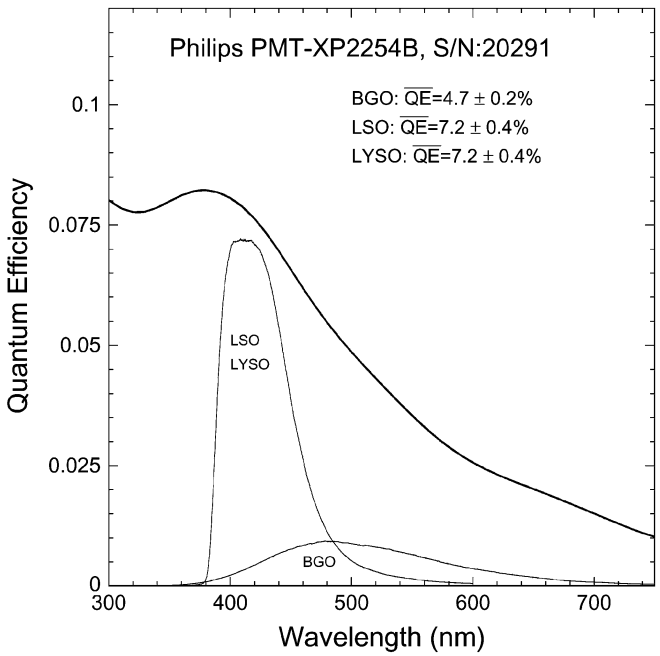

Fig. 5. Quantum efficiency of the XP2254b PMT (the thick solid line) is shown as function of wavelength together with the emission spectra of the LSO/LYSO and BGO samples, where the area under the emission curves is roughly proportional to corresponding absolute light output.

samples as well as the emission weighted average quantum efficiencies, which can be used to convert the measured photoelectron yield to the absolute light output in photon numbers. Taking into account the PMT response, we conclude that the light yield of the BGO sample is a factor of 4 lower that of the LSO and LYSO samples.

IV. Scintillation and Optical Properties of Long Samples

The excitation and emission spectra were measured at several locations for two long LYSO samples. No variation is observed, indicating a consistent scintillation mechanism along these samples. Fig. 6 shows the longitudinal and transverse transmittance spectra measured for two long LYSO samples. Once again, no variation is observed in the transverse transmittance spectra measured at three locations along these two samples. While the transverse transmittance measured for the Saint-Gobain sample approaches the theoretical limit calculated according to (1) by using the refractive index data from

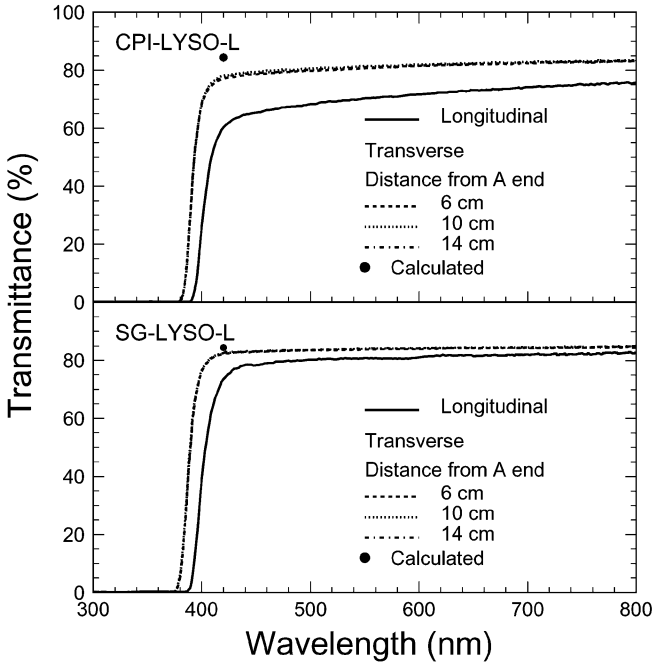

Fig. 6. Longitudinal and transverse transmittance spectra measured at three locations are shown as a function of wavelength for the CPI and the Saint-Gobain long LYSO samples, and compared to the calculated theoretical limit.

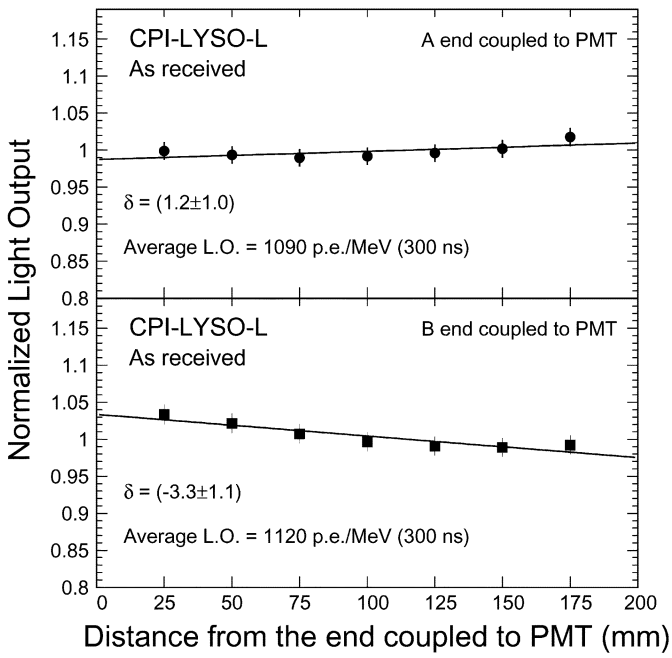

Fig. 7. Light response uniformities are measured with the (top) A and (bottom) B end coupled to the XP2254b PMT for the CPI long LYSO sample.

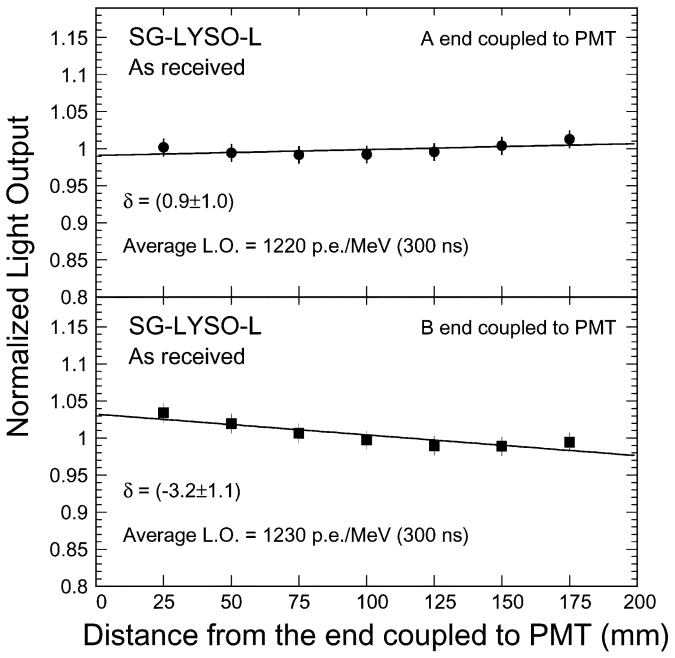

Fig. 8. Light response uniformities are measured with the the (top) A and (bottom) B end coupled to the XP2254b PMT for the Saint-Gobain long LYSO sample.

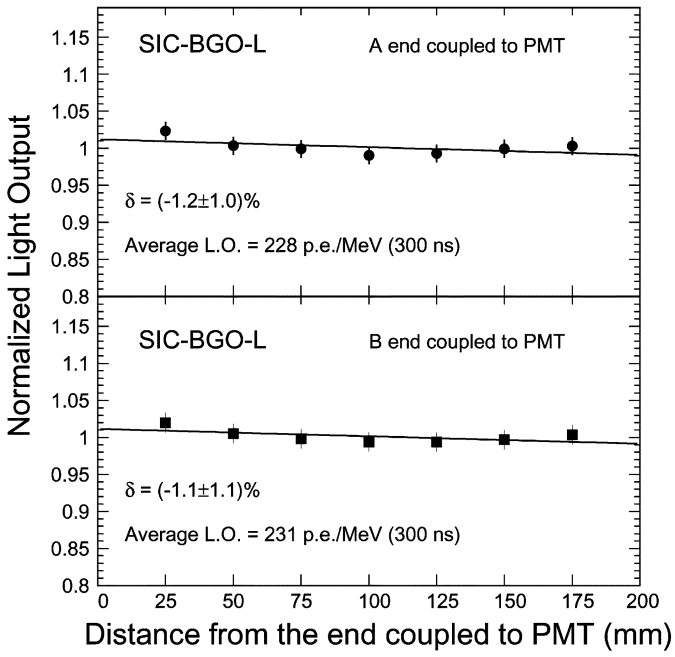

Fig. 9. Light response uniformities are measured with the (top) A and (bottom) B end coupled to the XP2254b PMT for the SIC long BGO sample.

[2], its longitudinal transmittance shows an absorption peak at 580 nm, which does not interfere with its emission so has no effect on its light output. An overall poorer transmittance was observed for the CPI sample, which apparently was caused by its poor surface polishing.

Figs. 7–9 show the light response uniformity measured using the XP2254b PMT and the corresponding linear fit to the (3) for three long samples. While the BGO sample shows a consistent slight negative δ when both the A and B end coupled to the PMT, two long LYSO samples show different sign of δ when the end

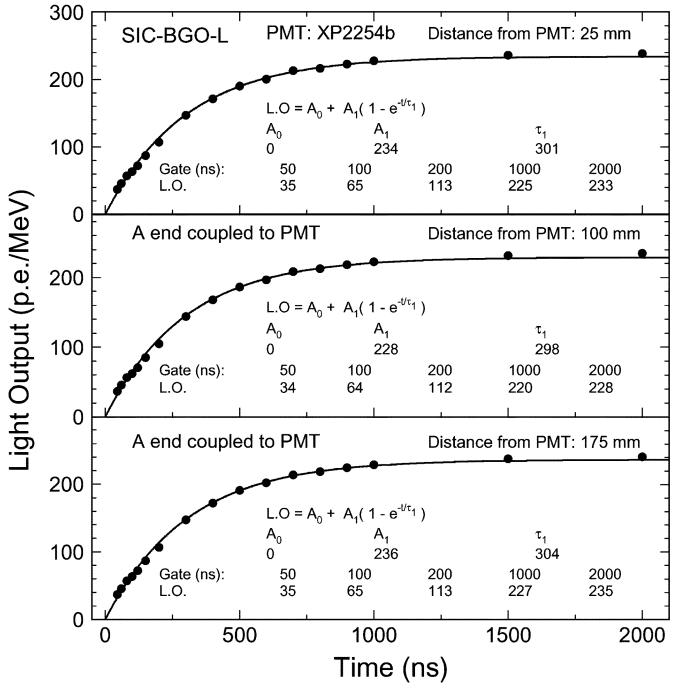

Fig. 10. Light output, measured at three locations, is shown as a function of the integration time for the SIC long BGO sample with the A end coupled to the XP2254b PMT.

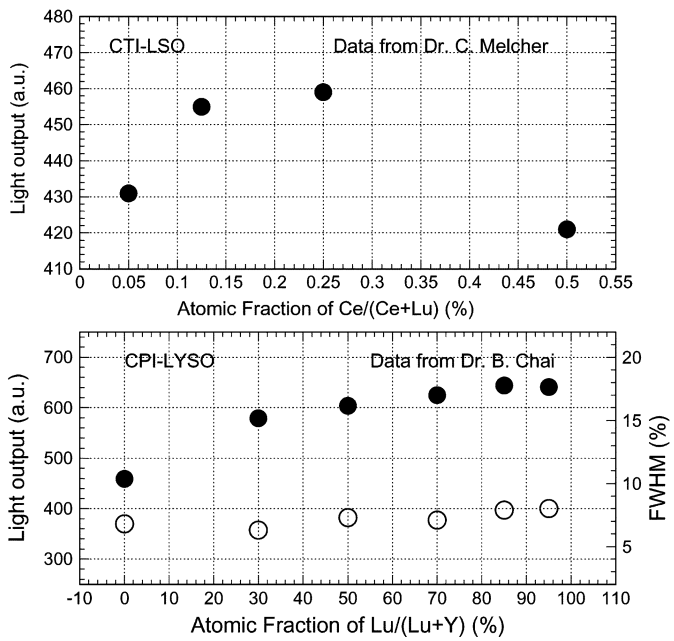

Fig. 11. Top plot: The light output is shown as a function of the cerium concentration in LSO [8]. Bottom plot: The light output (solid dots, left scale) and the energy resolution (open dots, right scale) of pixel size samples are shown as a function of the lutetium fraction in LYSO [6].

coupled to the PMT is switched. This observation hints a slight longitudinal nonuniformity of light yield along the axis of these long LYSO samples. The BGO sample, on the other hand, has a good longitudinal uniformity as shown in Fig. 10.

The origin of this difference can be attributed to their chemical nature. While BGO is an intrinsic scintillator, LYSO is a cerium doped scintillator. It is well known that the light output

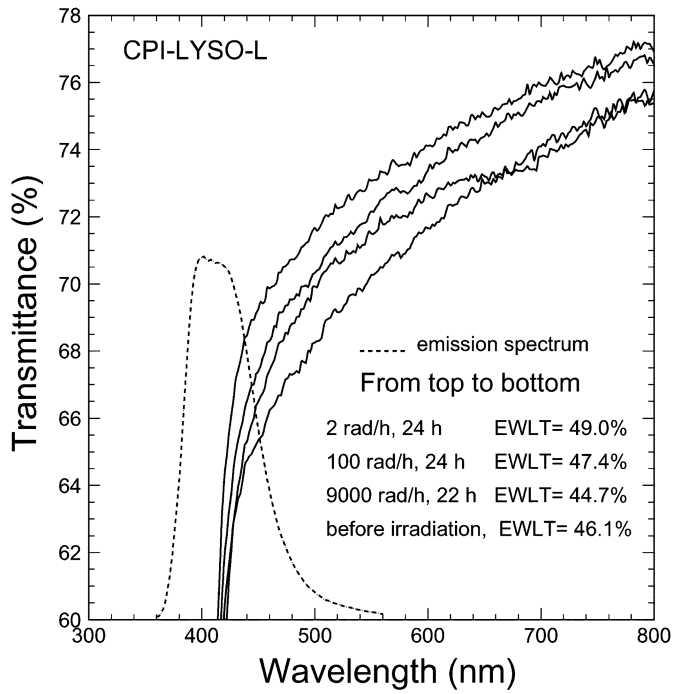

Fig. 12. Longitudinal transmittance spectra (solid curves) before and after 2, 100, and 9 000 rad/h irradiations and the emission spectrum (dashes) are shown as a function of wavelength for the CPI long LYSO sample.

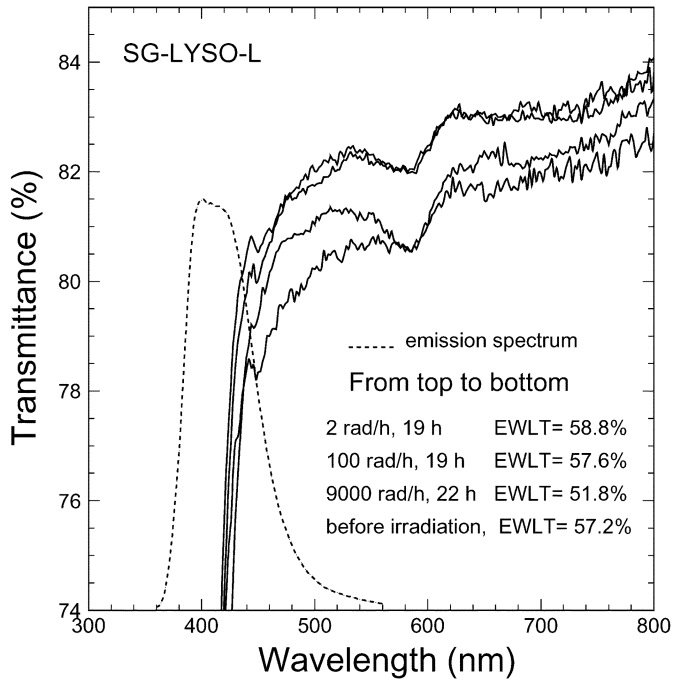

Fig. 13. Longitudinal transmittance spectra (solid curves) before and after 2, 100, and 9 000 rad/h irradiations and the emission spectrum (dashes) are shown as a function of wavelength for the Saint-Gobain long LYSO sample.

of these crystals is affected by both the cerium concentration and the yttrium fraction. The top plot of Fig. 11 shows the effect of the cerium concentration on crystal's light output [8]. The bottom plot of Fig. 11 shows both the light output and the energy resolution samples as a function of the lutetium fraction in LYSO samples of pixel size [6]. Any longitudinal variation of the cerium concentration and/or the yttrium fraction in LYSO

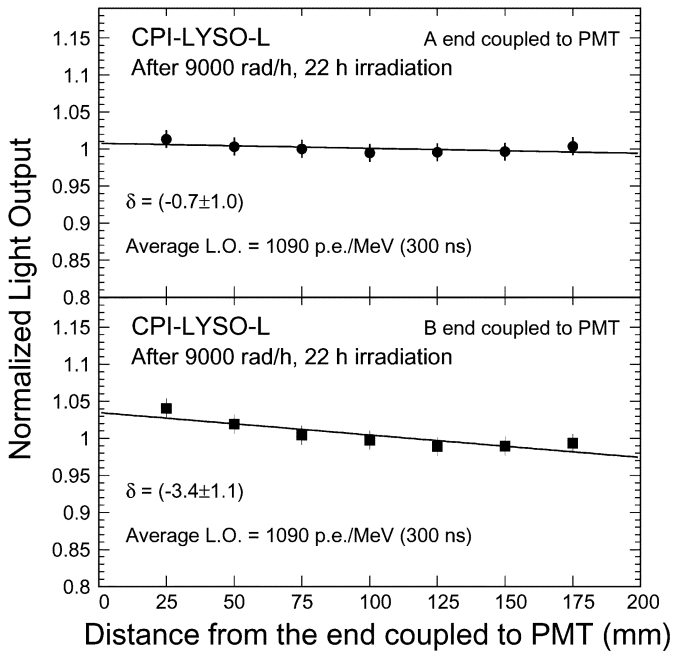

Fig. 14. Light response uniformities of the CPI long LYSO sample measured after 22 h irradiation at 9 000 rad/h with the (top) A and (bottom) B end coupled to the PMT.

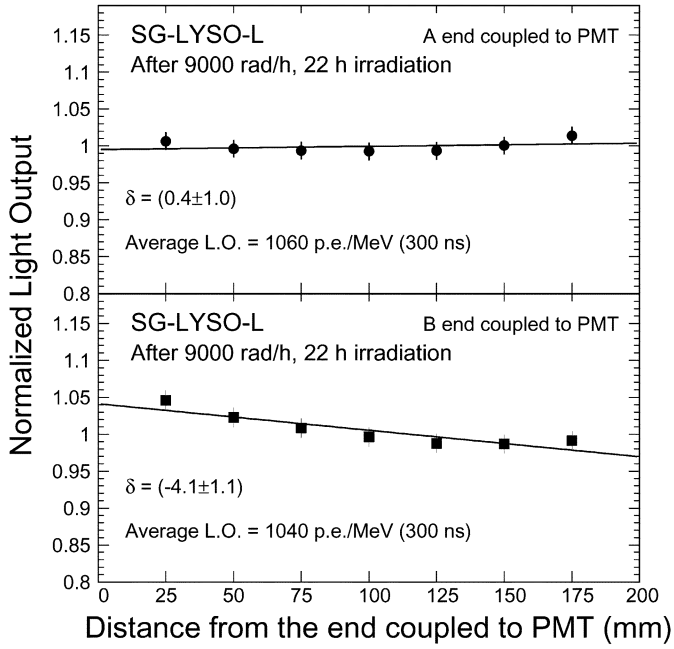

Fig. 15. Light response uniformity of the Saint-Gobain long LYSO sample measured after 22 h irradiation at 9 000 rad/h with the (top) A and (bottom) B end coupled to the PMT.

thus would certainly affect long sample's light response uniformity. To achieve and maintain the excellent energy resolution promised by a crystal calorimeter, effort must be made to develop long crystals of consistent light response uniformity, even under irradiations [11].

V. Radiation Damage in Long LYSO Samples

All known crystal scintillators suffer from radiation damage. Crystal radiation damage appears in the radiation induced ab-

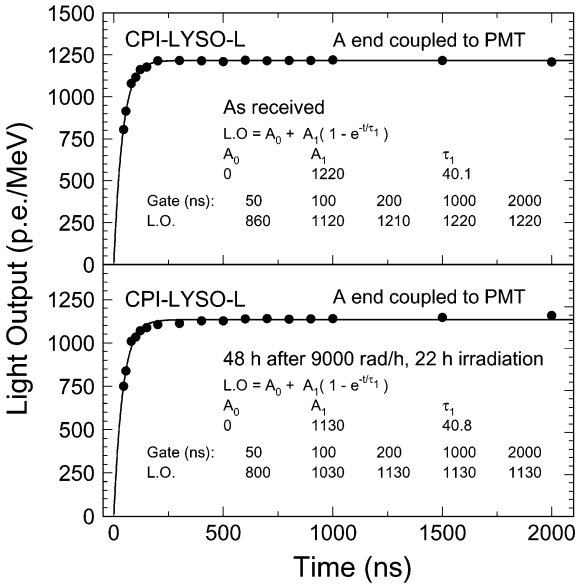

Fig. 16. Comparison of the decay kinetics before and after 22 h irradiation at 9 000 rad/h for the CPI long LYSO sample with the A end coupled to the PMT.

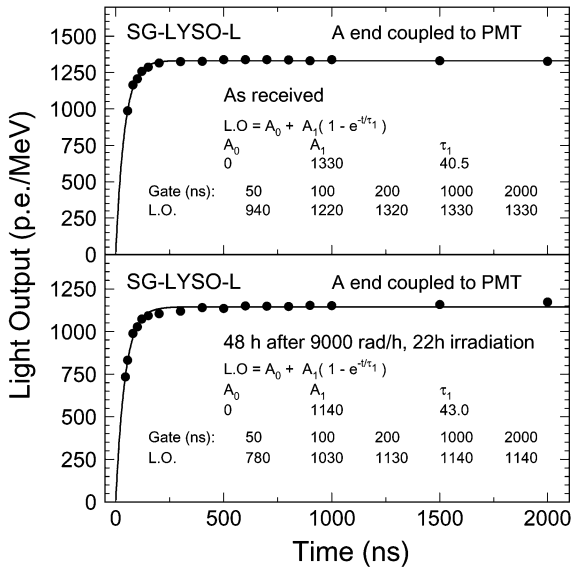

Fig. 17. Comparison of the decay kinetics before and after 22 h irradiation at 9 000 rad/h for the Saint-Gobain long LYSO sample with the A end coupled to the PMT.

sorption (color center formation), a reduced scintillation light yield (damage of the scintillation mechanism) or the radiation induced phosphorescence (afterglow). While the damage to the absorption or scintillation light yield may lead to a reduction of the light output or a deformation of the light response uniformity, the radiation induced phosphorescence would lead to an increase of the readout noise.

The excitation and emission spectra were measured for two long LYSO samples after 22 h irradiations at 9 000 rad/h. No variation is observed when compared to that measured before irradiations, indicating no damage in the scintillation mechanism. Figs. 12 and 13 show an expanded view of the longitudinal transmittance spectra measured for two long LYSO samples before and after each step of γ-ray irradiations at 2, 100, and 9 000

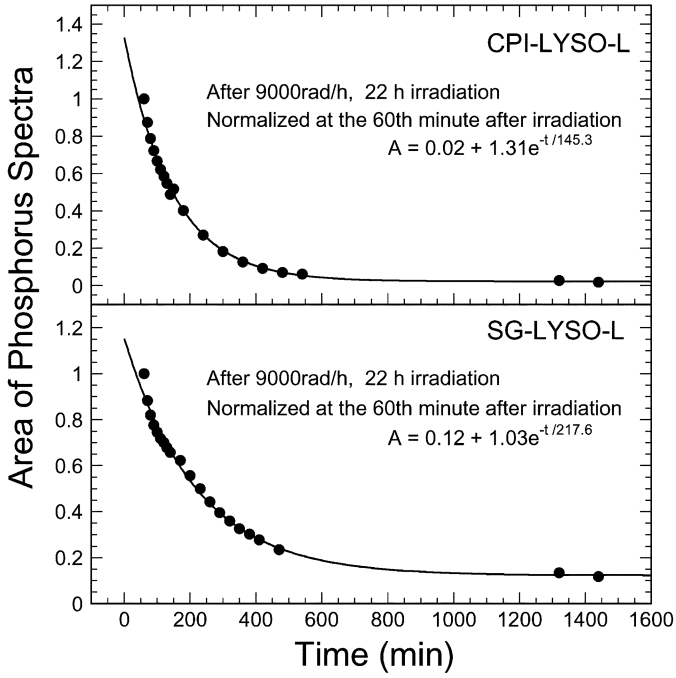

Fig. 18. Amplitude of phosphorescence is shown as a function of time after 22 h irradiation at 9 000 rad/h for the (top) CPI and (bottom) Saint-Gobain long LYSO samples.

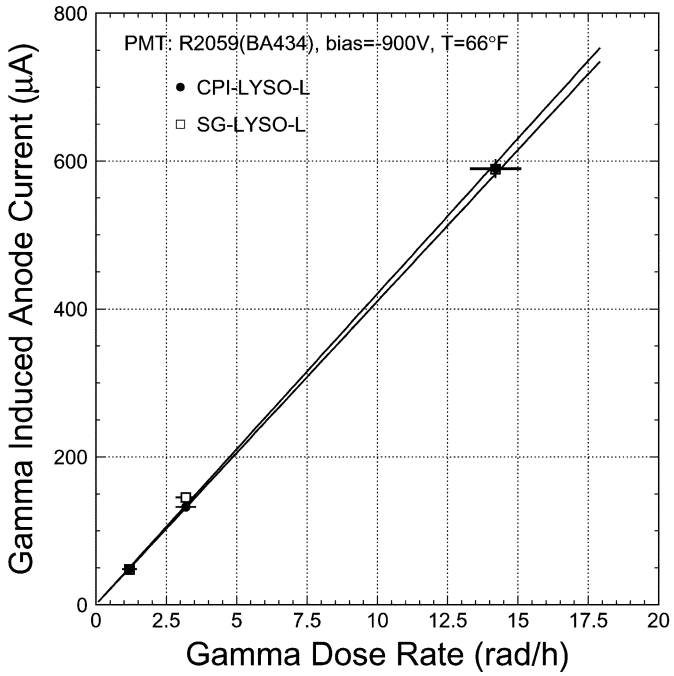

Fig. 19. γ-ray induced anode current is shown as a function of the dose rate for the CPI and Saint-Gobain long LYSO samples.

rad/h. An immediate increase of the longitudinal transmittance after the first irradiation under 2 rad/h was observed, which was followed by some degradation under higher dose rate. The numerical values of the emission weighted longitudinal transmittance (EWLT), which is defined as

$$\mathrm{EWLT} = \frac{\int \mathrm{LT}(\lambda)\mathrm{EM}(\lambda)\, d\lambda}{\int \mathrm{EM}(\lambda)\, d\lambda} \tag{4}$$

TABLE III
γ-RAY INDUCED READOUT NOISE IN TWO LONG LYSO SAMPLES

Sample ID	L.Y. p.e./MeV	F μA rad^{-1}h	Q_{15} p.e.	Q_{500} p.e.	σ_{15} MeV	σ_{500} MeV
CPI	1,480	41	6.98×10^4	2.33×10^6	0.18	1.03
Saint-Gobain	1,580	42	7.15×10^4	2.38×10^6	0.17	0.97

are also shown in these figures. The amplitude of the observed EWLT variations is smaller than crystal scintillators commonly used in experimental physics [11], indicating that the radiation induced absorption is a minor effect.

Figs. 14 and 15 show light response uniformity measured after the 9 000 rad/h irradiation and the corresponding linear fit to the (3) for the CPI and Saint-Gobain long LYSO samples. Compared to Figs. 7 and 8, some degradations in both the slope (δ) and the average light output $(\mathrm{LO_{mid}})$ are observed after irradiations, which are caused by the radiation induced absorption. Figs. 16 and 17 compare the light output and the decay kinetics before and after 22 h irradiations at 9 000 rad/h for two long LYSO samples. While some degradation of light output is observed, the decay time remains stable for both samples.

The radiation induced phosphorescence spectra of the CPI and Saint-Gobain long LYSO samples were continuously measured for more than 48 h after 22 h irradiations at 9 000 rad/h. No variation of the phosphorescence spectra were observed for both samples. The amplitude of phosphorescence, normalized to 1 h after the end of the irradiation, were fit to an exponential function

$$A = A_0 + A_1 e^{-t/\tau}. \tag{5}$$

Fig. 18 shows the fit result. The decay time constants of the radiation induced phosphorescence were determined to be 2.5 h and 3.6 h respectively for the CPI and the Saint-Gobain samples. The Saint-Gobain sample is also noticed to have a slightly larger residual phosphorescence. To evaluate the radiation induced phosphorescence related readout noise, the Hamamatsu R2059 PMT was used to measure the γ-ray induced anode current for these LYSO samples under γ-ray irradiations at 1.2, 3.2, and 14.2 rad/h. Fig. 19 shows the result of this measurement and a linear fit. These two samples have overall compatible radiation induced phosphorescence. Table III summarizes the result, where LY is the photoelectron yield of the sample as measured by the R2059 PMT. F is the γ-ray induced anode current per unit dose rate from the fit. Q_{15} and Q_{500} are the induced photoelectron numbers in 100 ns gate for these two samples under 15 and 500 rad/h respectively, which were calculated by using the F and the corresponding gain of the R2059 with 900 V bias, σ_{15} and σ_{500} are the corresponding energy equivalent readout noise, which were derived as the r.m.s. fluctuation of the photoelectron numbers. The radiation induced phosphorescence related readout noise is estimated to be about 1 MeV equivalent with 100 ns integration time for these two long LYSO samples under 500 rad/h.

VI. SUMMARY

Ce doped LSO and LYSO crystals have identical emission, excitation and transmittance spectra. The amplitude of their fast scintillation light of 42 ns decay time is about 4 times of BGO with 300 ns decay time. The absorption edge in their transmittance spectrum affects their light output. One approach to increase their light output is to improve their absorption edge toward a shorter wavelength. Large size ($2.5 \times 2.5 \times 20$ cm) LYSO samples from CPI and Saint-Gobain have good overall longitudinal uniformity in optical and scintillation properties. Their light response uniformity, however, may slightly affected by the distribution of the Ce concentration [8] or the yttrium fraction in the LYSO samples [6].

Radiation effect on transmittance, emission and light output in LYSO samples is small as compared to other commonly used crystal scintillators. Radiation induced phosphorescence in LYSO has a decay time constant of 2.5 to 3 h. The γ-ray induced phosphorescence related readout noise for 100 ns integration time is about 1 MeV equivalent, estimated for $2.5 \times 2.5 \times 20$ cm LYSO samples in an radiation environment of 500 rad/h.

In a brief summary, with existing mass production capabilities LSO and LYSO crystals are a good candidate for applications in high energy and nuclear physics. Further investigation, however, is needed to understand the performance of these long samples with solid state device, such as Si PD or APD, readout.

ACKNOWLEDGMENT

The authors would like to thank Dr. B. Chai, Dr. C. Melcher, and Dr. D. Rothan for many useful discussions. Dr. B. Chai and Dr. C. Melcher provided data presented in Fig. 11 of this paper.

REFERENCES

[1] K. Takagi and T. Fakazawa, "Cerium activated Gd_2SiO_5 single crystal scintillator," *Appl. Phys. Lett.*, vol. 42, pp. 43–45, 1983.
[2] C. Melcher and J. Schweitzer, "Cerium-doped lutetium oxyorthosilicate: A fast, efficient new scintillator," *IEEE Trans. Nucl. Sci.*, vol. 39, no. 2, pp. 502–505, Apr. 1992.
[3] D. W. Cooke, K. J. McClellan, B. L. Bennett, J. M. Roper, M. T. Whittaker, and R. E. Muenchausen, "Crystal growth and optical characterization of cerium-doped $Lu_{1.8}Y_{0.2}SiO_5$," *J. Appl. Phys.*, vol. 88, pp. 7360–7362, 2000.
[4] T. Kimble, M. Chou, and B. H. T. Chai, "Scintillation properties of LYSO crystals," presented at the IEEE Nuclear Science Symp. Conf., 2002.
[5] W. Wisniewski, "Consideration for calorimetry at a super B factory," in *Proceedings of Tenth International Conference on Calorimetry in Particle Physics*, R.-Y. Zhu, Ed.. Singapore, 2002.
[6] B. Chai, private communication.
[7] D. Rothan, private communication.
[8] C. Melcher, private communication.
[9] D. A. Ma and R. Y. Zhu, "Light attenuation length of barium fluoride crystals," *Nucl. Instrum. Meth. A*, vol. 333, pp. 422–424, 1993.
[10] X. Qu *et al.*, "A study on yttrium doping in lead tungstate," *Nucl. Instrum. Meth. A*, vol. 480, pp. 470–487, 2002.
[11] R.-Y. Zhu, "Radiation damage in scintillating crystals," *Nucl. Instrum. Meth. A*, vol. 413, pp. 297–311, 1998.